JCSE The Journal of Corrosion Science and Engineering

ISSN 1466-8858 Volume 23, Paper 50 first submitted 21 September 2020
published 19 September 2021

Electrochemical and theoretical studies on protective film formed by a synthesized Schiff base on mild steel surface in acid media

G.PANDIMUTHU,[1,2] S.RAMESHKUMAR,[3] orcid.id:0000-0002-3044-6594
K.PARAMASIVAGANESH [2] orcid.id:0000-0001-5838-878X, **A.SANKAR[1#]** orcid.id:0000-0001-5456-4854

1. **Department of Chemistry, Kandaswami Kandar's College, P.Velur, Namakkal. Tamilnadu, India.**
2. **Department of Chemistry, Arumugam Pillai Seethai Ammal College,Tiruppatur, Sivagangai. Tamilnadu, India.**
3. **Department of Chemistry, Sri Vasavi College, Erode, Tamilnadu, India.**

 # Corresponding Author: sanvishnu2010@gmail.com

Abstract:

The Schiff base, N-((1H-indol-3-yl)methylene)-2,3dihydrobenzo[b][1,4]dioxin-6-amine (BIS) has been synthesized and its corrosion inhibition property on the corrosion of mild steel in 1.0 M HCl and 0.5 M H_2SO_4 media was studied by weight loss and electrochemical methods. The experimental results revealed that the corrosion inhibition efficiency increased with the concentration of inhibitor and exhibits higher corrosion inhibition efficiency in 1.0 M HCl solution than in 0.5 M H_2SO_4 solution. Tafel polarization curves showed that the Schiff base is mixed type inhibitor. The adsorption of the compound on the mild steel surface obeyed Langmuir adsorption isotherm. Corrosion inhibition mechanism was proposed based on the measurement of potential of zero charge and adsorption isotherm studies in the acid media. Effect of temperature on corrosion inhibition was studied using electrochemical impedance spectroscopy. The surface morphology of mild steel surface was analyzed using SEM and AFM techniques. Quantum chemical parameters of Schiff base molecules and its protonated form have also been derived and discussed.

Key words:

Schiff base; corrosion inhibition; electrochemical studies; adsorption isotherm; potential of zero charge.

JCSE The Journal of Corrosion Science and Engineering
ISSN 1466-8858 Volume 23, Paper 50 first submitted 21 September 2020
published 19 September 2021

1. INTRODUCTION

Metals and alloys are used in many industries. They undergo corrosion mostly by electrochemical reaction with the environment. Carbon steel an alloy of iron is used in many industries for different applications, which is susceptible to acid corrosion [1]. The use of corrosion inhibitors for the control of corrosion of metals and alloys in corrosive media has become one of the best-known methods [2,3]. Various types of organic compounds have been reported in the literature as potential corrosion inhibitors [4-11]. Organic compounds with the hetero atoms N,O,S or P are shown to function as effective corrosion inhibitors [12-18]. The effect of organic nitrogen compounds as corrosion inhibitors on the corrosion of mild steel in acid media was analyzed and their rapid corrosion inhibition was reported [4,7,11]. The corrosion inhibition performance of the organic compounds is related to their adsorption properties [19]. Compounds containing π electrons were also reported to function as effective corrosion inhibitors [20-22]. In the view of above discussion an attempt was made to explore the corrosion inhibition performance of a synthesized Schiff base, N-((1H-indol-3-yl)methylene)-2,3dihydrobenzo[b][1,4]dioxin-6-amine (BIS) in controlling corrosion of mild steel in acid media, employing weight loss, electrochemical impedance and potentiodynamic polarization studies. This compound contains the hetero atoms nitrogen and oxygen and >C=N- group in addition to aromatic rings. The lone pair of electrons on the N atom and π electrons of >C=N- group and aromatic rings can be used to form bonding with surface iron atoms of mild steel in acid media. The corrosion inhibition mechanism was further analyzed using adsorption isotherm, potential of zero charge and temperature studies.

2. EXPERIMENTAL METHODS

2.1 MATERIALS

Mild steel specimens, cut from a mild steel plate, of composition 0.092% C, 0.032% Mn, 0.029% P, 0.022% S and rest Fe and dimensions 2.5 cm, 1.0 cm and 0.1 cm have been used for weight loss studies. The mild steel specimens were taken in the form of coupons with a hole of 2.5 mm, through which they are inserted into the glass hooks immersed in the acid media. A heated cylindrical carbon steel rod of same composition (verified by Optical Emission Spectroscopy), was coated with PTFE by inserting into the cylindrical PTFE block. The bottom of the rod has an exposed area of 0.2826 cm^2, which was used for electrochemical studies. The length of the PTFE coated rod is 24 cm, and 20 cm from the bottom is completely coated with Teflon. Mild steel coupons and the exposed area

JCSE The Journal of Corrosion Science and Engineering
ISSN 1466-8858 Volume 23, Paper 50 first submitted 21 September 2020
published 19 September 2021

of cylindrical rod were polished mechanically using emery sheets of grade 120, 200, 400, 600, 800 and 1200 and then washed thoroughly with double distilled water, degreased with acetone and dried. The solutions of 1.0 M HCl and 0.5 M H_2SO_4 were prepared from the analytical grade reagents using double distilled water. The inhibitor solutions were prepared in 1.0 M HCl and 0.5 M H_2SO_4 solutions. 3% ethanol by volume was added to acid solutions for the solubility reasons of inhibitor.

2.2 SYNTHESIS OF SCHIFF BASE

The precursors 2,3-dihydrobenzo[b][1,4]dioxin-6-amine (>98%) and Indole-3-carbaldehyde (>97%) were purchased from Sigma Aldrich and dissolved in minimum amount of ethanol separately in 1:1 mole ratio and then these solutions were mixed in a round bottom flask fitted with an air condenser. The mixture is refluxed at 45°C for six hours and finally poured in ice cold water, a white coloured compound separated out. This solid is recrystallized using ethanol and used as corrosion inhibitor. The reaction scheme is shown in Figure 1. The formation of Schiff base was confirmed by the appearance of new peak for >C=N- in the Schiff base at 1726 cm-1 and disappearance of characteristics peaks for the functional groups in the starting materials. The FTIR spectrum of the synthesized Schiff base (BIS) is shown in Figure 2.

2.3 WEIGHT LOSS MEASUREMENTS

By adopting standard procedure prescribed by ASTM for Testing and Materials, the weight loss measurements have been carried out [23]. The mild steel specimens in the form of coupons, in triplicate were immersed in the inhibited and uninhibited 100 ml acid solutions at room temperature (30±1°C) and the weight losses were measured at four-time intervals (2h, 5h, 10h and 24h). The weight loss of specimens taken in triplicate are very close and the average weight loss was used to calculate the corrosion inhibition efficiency. From the weight of the specimens measured in the inhibited and uninhibited acid solutions before and after corrosion, the corrosion inhibition efficiency was calculated using the formula;

$$IE\% = \left(\frac{w-w'}{w}\right) X100 \qquad (1)$$

JCSE The Journal of Corrosion Science and Engineering
ISSN 1466-8858 Volume 23, Paper 50 first submitted 21 September 2020
published 19 September 2021

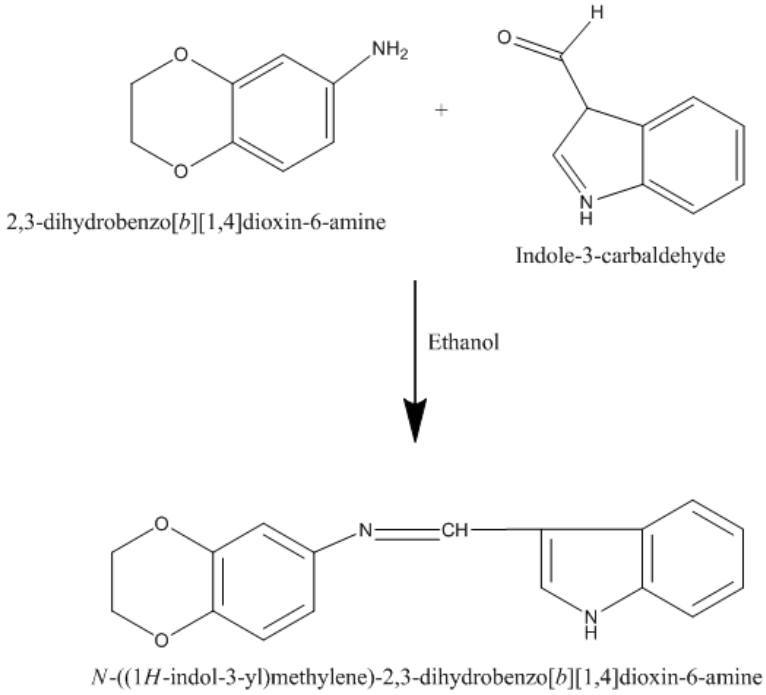

Fig.1 Reaction Scheme for Schiff base formation.

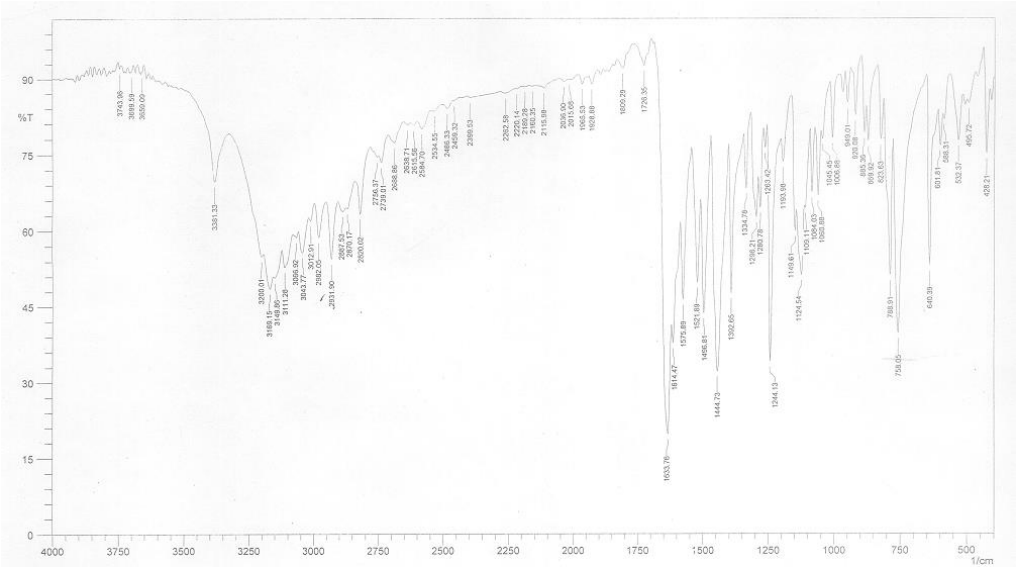

Fig. 2 FTIR Spectrum of BIS.

Where, W and W' are weight of the specimens in the absence and presence of inhibitor in acid solutions respectively. The average weight of triplicate specimens has been used for the weight loss measurement studies.

JCSE The Journal of Corrosion Science and Engineering
ISSN 1466-8858 Volume 23, Paper 50 first submitted 21 September 2020
published 19 September 2021

2.4 ELECTROCHEMICAL IMPEDANCE MEASUREMENTS

The electrochemical impedance spectra have been recorded for the corrosion of mild steel in the acid media in the absence and presence of BIS in the acid solutions using the Potentiostat/ Galvanostat/FRA (PARSTAT 2273, Princetone Applied Research, USA). The electrochemical impedance parameters were derived using PowerSuite, inbuilt software and analyzed using Zsimpwin Software (version 3.21). The impedance spectra were recorded using a three-electrode set up in the acid media, where a Pt foil served as counter electrode, a saturated calomel electrode performed as reference electrode. Teflon coated mild steel rod of above-mentioned composition was used as working electrode. Before recording the impedance spectra, the Teflon coated rod was immersed in the acid solution for 30 minutes to attain a stable value for corrosion potential. The impedance spectra were recorded in the AC frequency range 105 Hz to 0.01 Hz with an AC signal amplitude of 10mV at the corrosion potential. The experimental set up was made to measure four cycles for each frequency and ten frequencies were applied for each decade. From the Nyquist Plots the electrochemical parameters, double layer capacitance (Cdl) and charge transfer resistance (Rct) were obtained as described [24].The experimental curves were fitted with various equivalent circuits and the best fitting circuit was used to extract the electrochemical impedance parameters. Since the value of charge transfer resistance is inversely proportional to corrosion rate, the corrosion inhibition efficiency was calculated utilizing the expression:

$$IE\ \% = \frac{(R'_{ct} - R_{ct})}{R'_{ct}} \times 100 \qquad (2)$$

where R_{ct} and R'_{ct} are the charge transfer resistance in the absence and presence of inhibitor in the acid media.

2.5 POLARIZATION MEASUREMENTS

The Tafel polarization studies were carried out using the same cell set up employed for the measurements of impedance spectra. The potentials were swept at the scan rate of 1.66 mV/sec. This is primarily from a more negative potential than open circuit potential to a more positive potential than open circuit potential through corrosion potential. The Tafel region, where the linear fit can be observed, was found to be in the range -200 mV to -780 mV and hence the polarization plots were recorded in this range. From the plot of electrode potential vs log i, the corrosion potential (E_{corr}), the corrosion current density (i_{Corr}) and Tafel constants (β_a and β_c) were obtained in the presence and absence of inhibitor at various concentrations. These Tafel parameters were taken from an inbuilt

JCSE The Journal of Corrosion Science and Engineering
ISSN 1466-8858 Volume 23, Paper 50 first submitted 21 September 2020
published 19 September 2021

software in the powersuite software, which gave very good fitting. The corrosion current density is directly proportional to corrosion rate, corrosion inhibition efficiency was calculated utilizing the formula: [25]

$$IE\% = \frac{(i_{corr} - i'_{corr})}{i_{corr}} \times 100 \qquad (3)$$

where i_{corr} and i'_{corr} are corrosion current densities in the absence and presence of inhibitor respectively.

2.6 MEASUREMENT OF THE POTENTIAL OF ZERO CHARGE

The electrochemical impedance spectra were recorded at a fixed single frequency (200 Hz) for the inhibited and uninhibited acid solutions by superimposing the input AC sinusoidal voltage of small amplitude 10 mV at different DC potentials. A graph was plotted between applied DC potential and double layer capacitance to determine the potential of zero charge (PZC).

2.7 EFFECT OF TEMPERATURE

The effect of temperature on the corrosion of mild steel in acid media and corrosion inhibition performance of synthesized Schiff base was studied in the temperature range 303 – 323 K using electrochemical impedance spectroscopy with the same frequency range and amplitude.

2.8 COMPUTATIONAL PROCEDURE

Quantum chemical calculations were made for the protonated and neutral Schiff base molecules in gas phase without any symmetry constraints. The geometrical optimization was done using DFT at B3LYP hybrid basis functional set [26,27].

3.RESULTS AND DISCUSSION

3.1 WEIGHT LOSS MEASUREMENTS

The corrosion inhibition efficiency values evaluated from the weight loss measurements are presented in Table.1. From this table it is obvious that the corrosion inhibition efficiency increases with inhibitor concentration, this is attributed to the adsorption of Schiff base molecules onto the mild steel surface. The Schiff base molecules get adsorbed on the mild steel surface and cover maximum area, which was in direct contact with corrosive media and thus, the surface area of mild steel specimens in contact with the corrosive media decreases. The extent of surface coverage increases with the concentration of inhibitor. In both the acid media, we observed that there is no significant increase in corrosion inhibition efficiency beyond 600 ppm of inhibitor. Thus, the inhibitor exhibited maximum inhibition efficiency at 600 ppm concentration. The corrosion inhibition efficiency also increased with time to a smaller extent. From Table.1 it can also be seen that the corrosion inhibition

JCSE The Journal of Corrosion Science and Engineering
ISSN 1466-8858 Volume 23, Paper 50 first submitted 21 September 2020
published 19 September 2021

efficiency of the inhibitor is almost same in 1.0 M HCl than that in 0.5 M H_2SO_4 solution, there is no marked significant difference in corrosion inhibition efficiency. Hence, the corrosion inhibition efficiency of the Schiff base depends on the H^+ ion concentration only irrespective of the counter ion of acid.

Table.1 Corrosion inhibition efficiency of the Schiff base BIS on the corrosion of mild steel in1.0 M HCl and 0.5 M H_2SO_4 solutions from weight loss measurements.

Medium	Concentration of the Schiff base (ppm)	2 hours		5 hours		10 hours		24 hours	
		Corrosion rate (mmpy)	IE%	Corrosion rate (mmpy)	IE%	Corrosion rate (mmpy)	IE%	Corrosion rate (mmpy)	IE%
1.0 M HCl	Blank	183		268		337		821	
	50	51.6	71.8	77.0	72.4	90.3	73.2	218	73.5
	100	44.4	75.7	63.5	76.3	76.8	77.2	207	74.8
	200	38.9	78.7	55.5	79.3	66.1	80.4	159	80.7
	400	30.1	83.6	42.1	84.3	50.9	84.9	122	85.2
	600	23.9	86.9	34.3	87.2	40.1	88.1	95.2	88.4
	800	23.7	87.0	34.5	87.1	40.5	87.9	95.5	88.3
	1000	23.8	86.9	34.5	87.1	40.2	88.1	95.7	88.3
0.5 M H_2SO_4	Blank	296		318		467		982	
	50	86.7	70.7	89.0	72.0	129	72.4	266	72.9
	100	76.3	74.2	78.9	75.2	112	76.1	229	76.7
	200	69.3	76.6	72.2	77.3	103	77.9	210	78.6
	400	58.9	80.1	59.8	81.2	82.2	82.4	169	82.8
	600	46.7	84.2	43.3	86.4	58.4	87.5	119	87.9
	800	46.4	84.3	43.2	86.4	58.3	87.5	117	88.1
	1000	46.1	84.4	43.4	86..3	58.4	87.5	118	87.9

JCSE The Journal of Corrosion Science and Engineering
ISSN 1466-8858 Volume 23, Paper 50 first submitted 21 September 2020
published 19 September 2021

3.2 ELECTROCHEMICAL IMPEDANCE SPECTROSCOPY

The corrosion inhibition performance of the synthesized Schiff base on the corrosion of mild steel in 1.0 M HCl and 0.5 M H_2SO_4 solutions has also been evaluated using electrochemical impedance spectroscopy. The impedance spectra recorded for the corrosion of mild steel in the acid media in the absence and presence of inhibitor molecules are shown in Fig.3a and 3b.

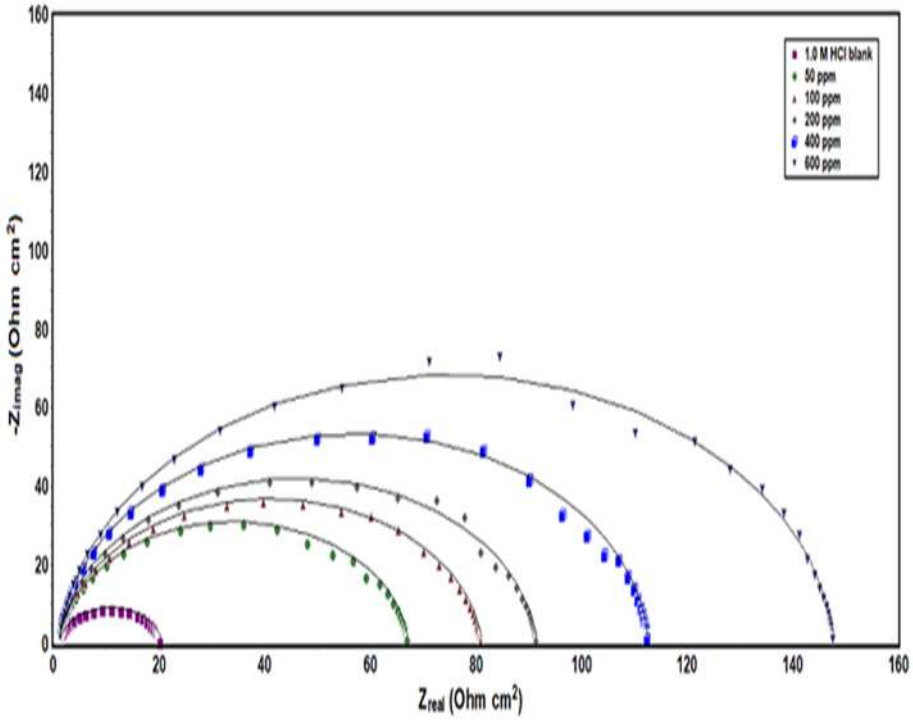

Fig.3a Nyquist plots recorded for the corrosion of mild steel in 1.0 M HCl solutions in the absence and presence of BIS at various concentrations.

JCSE The Journal of Corrosion Science and Engineering
ISSN 1466-8858 Volume 23, Paper 50 first submitted 21 September 2020
published 19 September 2021

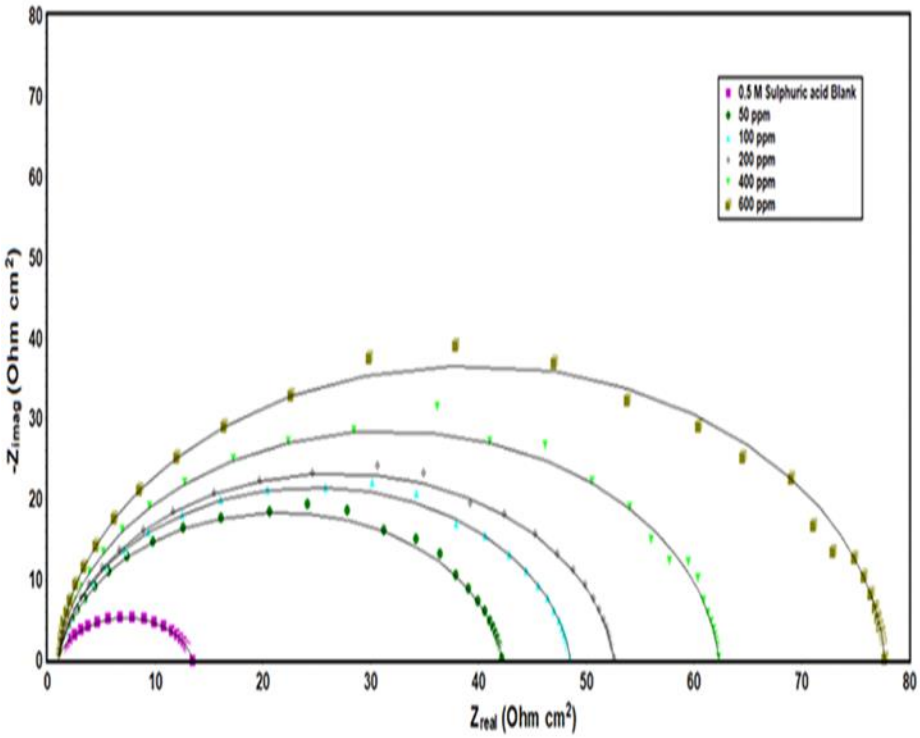

Fig.3b Nyquist plots recorded for the corrosion of mild steel in 0.5 M H_2SO_4 solutions in the absence and presence of BIS at various concentrations.

Generally, the Nyquist plots obtained are not straight forward; we can't get the values for electrochemical impedance parameters from the plots directly. To extract the electrochemical impedance parameters from the plots equivalent circuits are used. The equivalent circuit which fits well with the experimental curves is found and used to extract the impedance parameters. In the present case, the experimental curves fitted well with an equivalent circuit shown in Fig.4. This equivalent circuit is called simple Randle's circuit and represented as – R (CR) – model. From Fig.3a and 3b, it is obvious that the experimental impedance curves are semi circles with depressed nature. This can be attributed to the non-ideal capacity behavior of mild steel- acid media interface [27-29]. Dispersion of double layer capacitance at the metal solution interface is due to the surface roughness, the degree of poly crystallinity, the chemical in homogeneities and anion adsorption [20,22]. A precise modelling for this phenomenon is expressed by introducing a constant phase element (CPE) in the place of capacitor [20,22] and the corresponding equivalent circuit is shown in Fig.4.

JCSE The Journal of Corrosion Science and Engineering
ISSN 1466-8858 Volume 23, Paper 50 first submitted 21 September 2020
published 19 September 2021

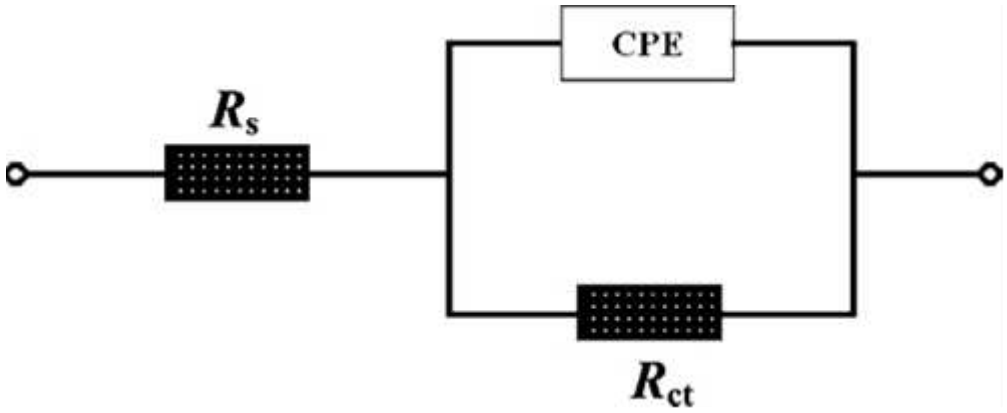

Fig.4.Equivalent circuit for the mild steel surface/corrosive media interface with CPE.

The electrochemical impedance parameters obtained by fitting the equivalent circuit with the experimental Nyquist plots for the corrosion of mild steel in acid media in the absence and presence of the Schiff base molecules are presented in Table.2. From this table it is also clear that the charge transfer resistance (R_{ct}) value increases and the double layer capacitance (C_{dl}) decreases with inhibitor concentration. This is due to the effective adsorption of inhibitor molecules onto mild steel surface. The double layer capacitance of the mild steel was calculated from the admittance (Y_0) and CPE parameter (n) as follows,

$$C_{dl} = Y_0 \omega^{n-1} \quad (4)$$

Where ω is the angular frequency found at the maximum value of imaginary part of measured impedance. Increase in surface coverage of the inhibitor molecules with concentration is revealed by increase in the R_{ct} values with inhibitor concentration (Figure.3a and 3b); this is attributed for increase in inhibitor efficiency [30-32]. The C_{dl} value decreases with the inhibitor concentration.

JCSE The Journal of Corrosion Science and Engineering
ISSN 1466-8858 Volume 23, Paper 50 first submitted 21 September 2020
published 19 September 2021

Table.2 Electrochemical impedance parameters for the corrosion of mild steel in 1.0 M HCl and 0.5 M H_2SO_4 solutions in the absence and presence of BIS at various concentrations.

Medium	Concentration of the Schiff base (ppm)	R_{ct} (Ohm cm^2)	n	C_{dl} (µF cm^{-2})	Inhibition Efficiency (%)	Surface Coverage (θ)
1.0 M HCl	Blank	19.1	0.912	173	-	-
	50	66.0	0.941	122	71.1	0.711
	100	80.1	0.933	94	76.2	0.762
	200	90.3	0.941	72	78.8	0.788
	400	111.4	0.962	51	82.9	0.829
	600	146.6	0.947	39	87.0	0.870
0.5 M H_2SO_4	Blank	12.5	0.909	207	-	-
	50	41.2	0.932	154	69.7	0.697
	100	47.5	0.939	116	73.7	0.737
	200	51.6	0.937	97	75.8	0.758
	400	61.3	0.955	75	79.6	0.796
	600	76.7	0.972	51	83.7	0.837

This is due to the adsorption of BIS at the metal – solution interface with the replacement of adsorbed water molecules, which led to the decrease in local dielectric constant and/or an increase in the thickness of electrical double layer [23]. Hence, the decrease in C_{dl} values caused by the gradual displacement of H_2O molecules by the adsorption of Schiff base at the metal-solution interface increase the surface coverage [24].

3.3 POLARIZATION MEASUREMENTS

Tafel plots obtained for the corrosion of mild steel in 1.0 M HCl and 0.5 M H_2SO_4 solutions are shown in Figure 5a and 5b.

JCSE The Journal of Corrosion Science and Engineering
ISSN 1466-8858 Volume 23, Paper 50 first submitted 21 September 2020
published 19 September 2021

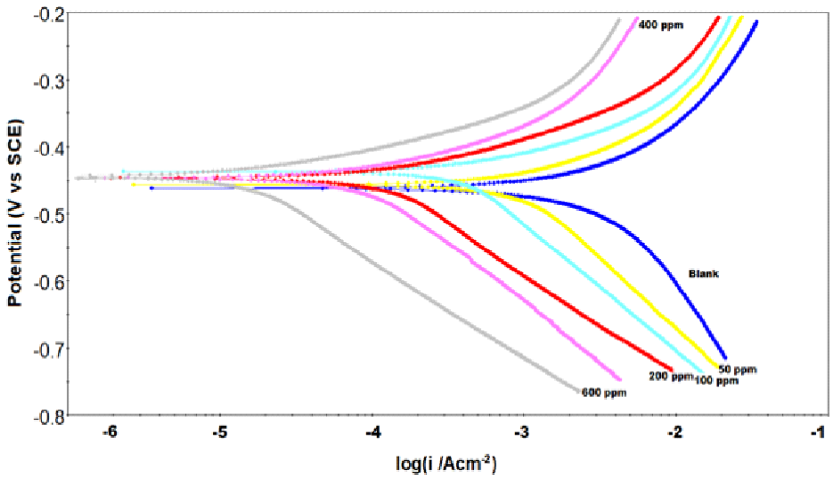

Fig.5a Tafel plots for the corrosion of mild steel in 1.0 M HCl solutions in the absence and presence of BIS at various concentrations.

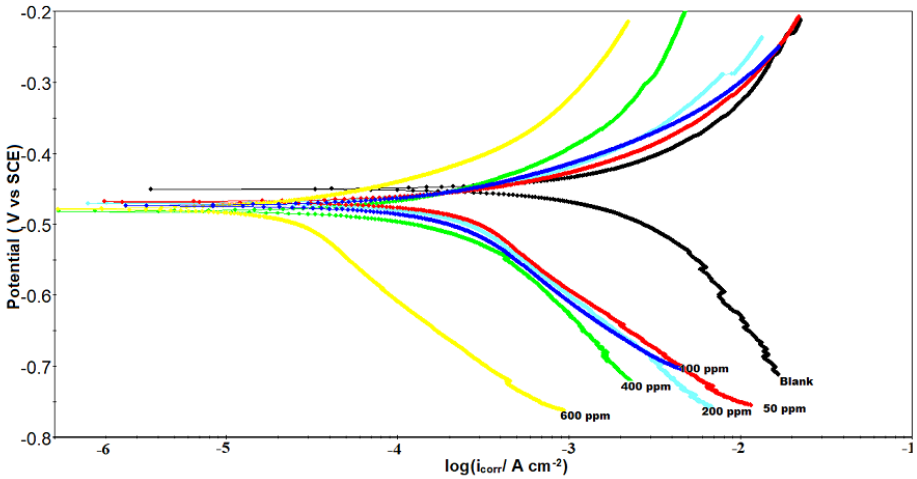

Fig.5b Tafel plots for the corrosion of mild steel in 0.5 M H_2SO_4 solution in the absence and presence of BIS at various concentrations.

From the Tafel plots it can be seen that the cathodic and anodic currents decrease with the addition of inhibitor to the acid solutions. Thus, BIS is of mixed type inhibitor. The low over potential region which is less than 50mV away from the E_{corr} can't used for the Tafel fit, because the Tafel equation considers anodic or cathodic reactions every time and generally the potential higher than the 50 mV from E_{corr} always satisfy the Tafel relation in most of the cases. i.e., A large difference between open circuit potential (OCP) values can be observed when the corrosive medium contains some reducible species, that can get reduced and deposited on the electrode surface in the cathodic region of the Tafel plot. Since, the surface is changed, the OCP of the new surface will be different from that of

JCSE The Journal of Corrosion Science and Engineering
ISSN 1466-8858 Volume 23, Paper 50 first submitted 21 September 2020
published 19 September 2021

the actual metal surface. When there is no a large change in Tafel constants, the corrosion mechanism is not changed in the presence of inhibitor and hence the surface of the metal is not changed. The potentiodynamic polarization parameters are presented in Table.3. From this table and Tafel plots, it is clear that the corrosion current density decreases with inhibitor concentration. From Table.3 it can be seen that the corrosion potential is shifted both in the anodic or cathodic directions with the addition of inhibitor to acid solutions in 1.0 M HCl solution and only in the cathodic direction in 0.5 M H_2SO_4 solution. However, the shift is not greater than 78mV on either direction. This also confirms the mixed type inhibition. Moreover, the values of βa and βc change 12 with the concentration of synthesized Schiff base. This shows the influence of the inhibitor in controlling corrosion both in the cathodic and anodic polarization plots.

Table.3 Tafel polarization parameters for MS in 1.0 M HCl and 0.5 M H_2SO_4 solutions in the presence and absence of BIS from Tafel polarization curves.

Medium	Concentration of the Schiff base (ppm)	E_{corr} (mV)	I_{corr} (mA cm^{-2})	β_a	β_c	Inhibition Efficiency (%)	Surface Coverage (θ)
1.0 M HCl	Blank	-450	1.17	110	257	-	-
	50	-450	0.427	102	212	70.8	0.708
	100	-428	0.373	109	218	75.1	0.751
	200	-446	0.334	116	223	77.9	0.779
	400	-445	0.306	101	203	81.9	0.819
	600	-448	0.289	99	217	86.1	0.861
0.5 M H_2SO_4	Blank	-455	2.930	143.9	245	-	-
	50	-457	1.163	97	132	69.1	0.691
	100	-461	1.005	105	131	73.2	0.732
	200	-460	1.888	94	129	75.4	0.754
	400	-478	0.809	89	125	78.8	0.788
	600	-475	0.768	92	137	83.2	0.832

3.4 POTENTIAL OF ZERO CHARGE AND THE CORROSION INHIBITION MECHANISM

JCSE The Journal of Corrosion Science and Engineering
ISSN 1466-8858 Volume 23, Paper 50 first submitted 21 September 2020
published 19 September 2021

The dependence of double layer capacitance on the applied DC potential is graphically represented in figure. 6a, 6b, 6c and 6d.

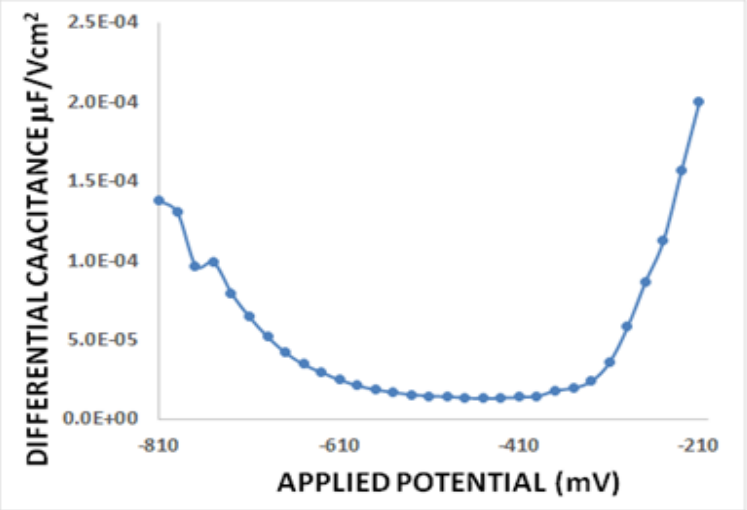

Fig.6a A plot of differential capacitance vs. applied electrode potential for mild steel in 1.0 M HCl solution.

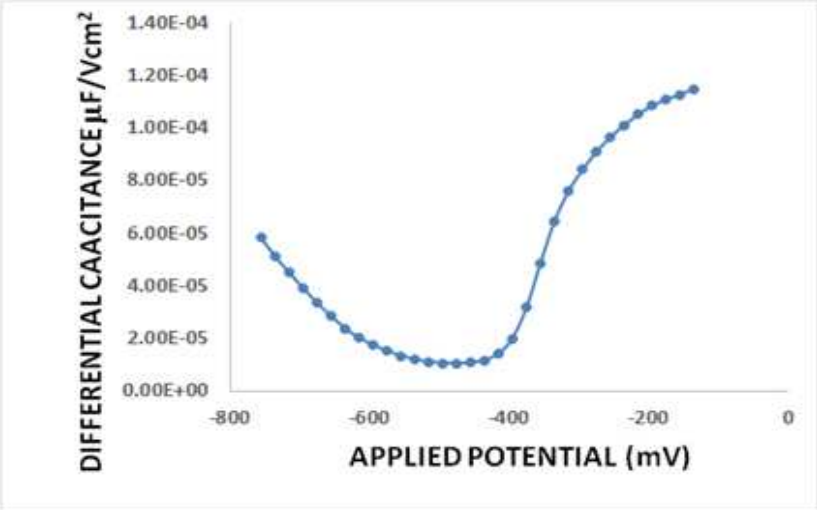

Fig.6b A plot of differential capacitance vs. applied electrode potential for mild steel in 0.5 M H_2SO_4solution.

JCSE The Journal of Corrosion Science and Engineering
ISSN 1466-8858 Volume 23, Paper 50 first submitted 21 September 2020
published 19 September 2021

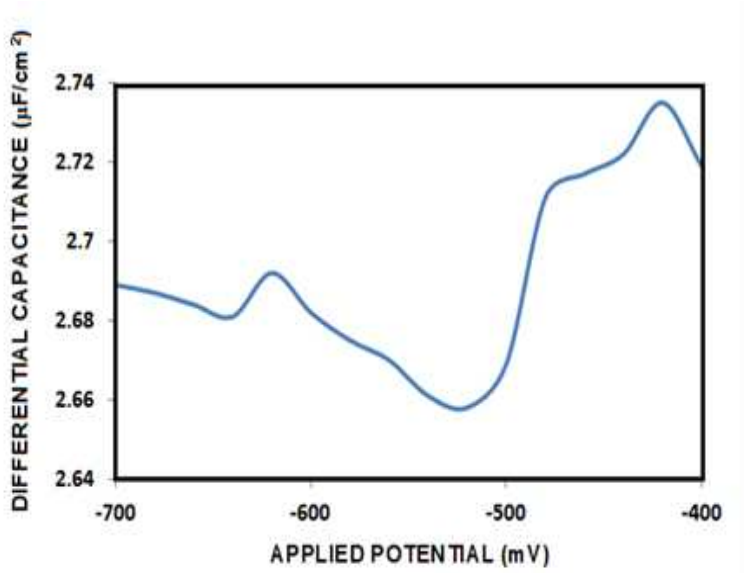

Fig.6c A plot of differential capacitance vs. applied electrode potential for mild steel in 1.0 M HCl solution containing 600 ppm of the BIS.

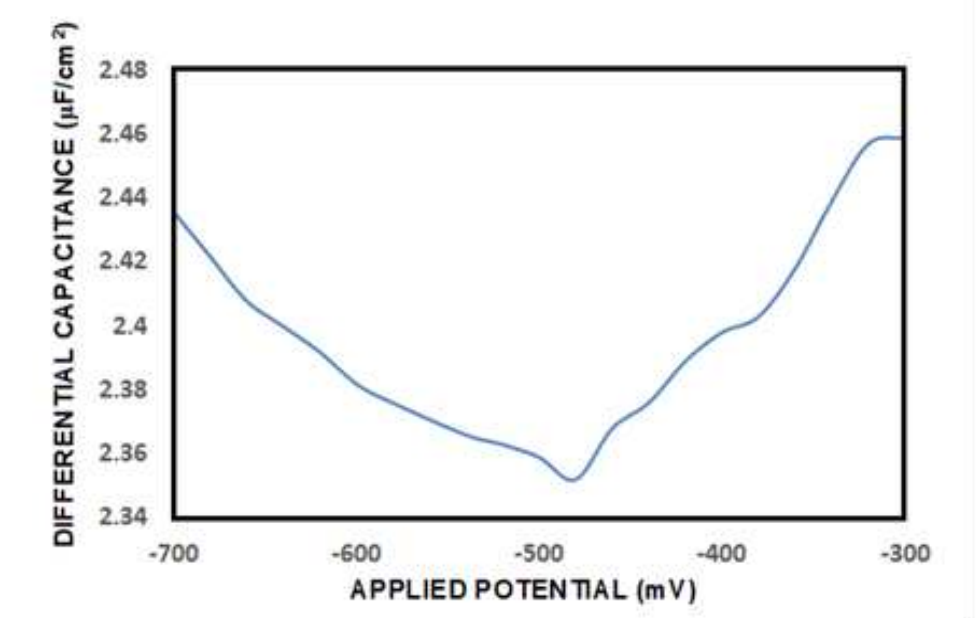

Fig.6d A plot of differential capacitance vs. applied electrode potential for mild steel in 0.5 M H_2SO_4 solution containing 600 ppm of the BIS.

JCSE The Journal of Corrosion Science and Engineering
ISSN 1466-8858 Volume 23, Paper 50 first submitted 21 September 2020
published 19 September 2021

The values PZC and E_{OCP} (open circuit potential) for mild steel in the inhibited and uninhibited solutions of 1.0 M HCl and 0.5 M H_2SO_4 are shown in Table.4.

At the open circuit potential, the surface charge of the mild steel in the corrosive media is determined utilizing the equation;

$$E_r = E_{OCP} - E_{PZC} \quad (5)$$

where E_r – Antropov's "rational" corrosion potential [27-32,34]

The surface charge of the mild steel at OCP was found to be positive in the inhibited and uninhibited, 1.0 M HCl and 0.5 M H_2SO_4 solutions with respect to PZC. In uninhibited acid solutions the anions from the acid get attached to the positively charged metal surface

Table.4 Excess charge on mild steel electrode in 1 M HCl and 0.5 M H_2SO_4 solutions in the presence and absence of inhibitor.

S.No.	Medium	E_{ocp} (mV)	PZC (mV)	Excess Charge
1	1.0 M HCl	-450	-520	+
2	1.0 M HCl + 600ppm of inhibitor	-466	-520	+
3	0.5 M H_2SO_4	-455	-480	+
4	0.5 M H_2SO_4+ 600ppm of inhibitor	-450	-480	+

The Schiff base molecules can exist in protonated form via protonation of the nitrogen atom in acid media through a complex equilibrium. The protonated Schiff base molecules can't get attached to the positively charged metal surface in acid media in the inhibited acid media. However, the anions from acid can get attached to the metal surface and will help to attach the positively charged Schiff base molecules from the solution i.e. the anions act as bridge. The non-protonated molecules tend to occupy the vacant adsorption sites (not covered by anions) on the metal surface. In the present case the Cl^- and SO_4^{2-} ions adsorbed on the metal surface and increases the negative charge on the surface

JCSE The Journal of Corrosion Science and Engineering
ISSN 1466-8858 Volume 23, Paper 50 first submitted 21 September 2020
published 19 September 2021

which is decreased by the adsorption of protonated Schiff base molecules through electrostatic attraction [32].

The corrosion inhibition mechanism could be explained by the following figures 7 and 7a.

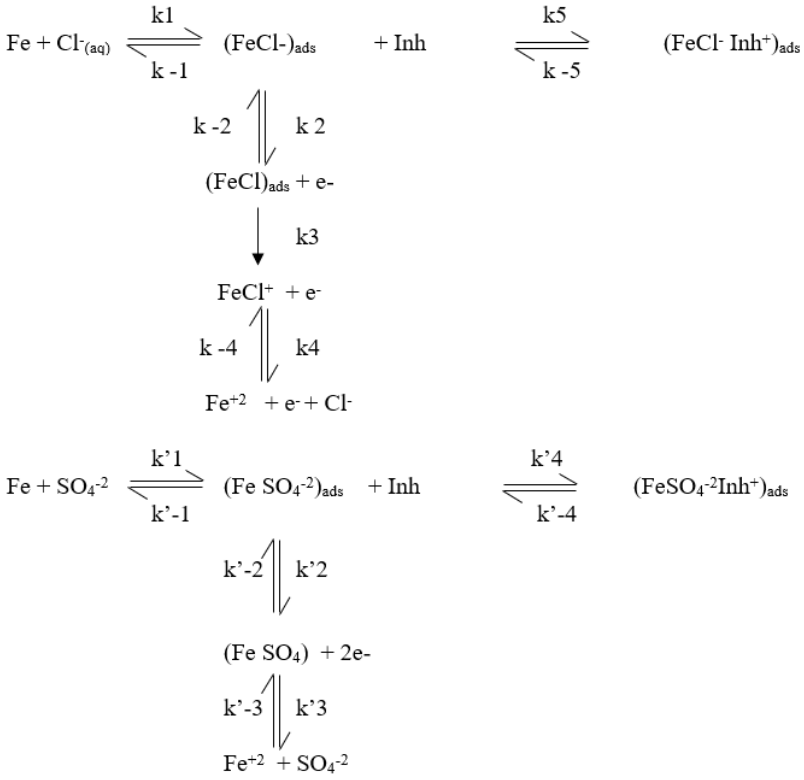

Fig.7 Adsorption of anions and protonated Schiff base molecules onto mild steel surface in acid media.

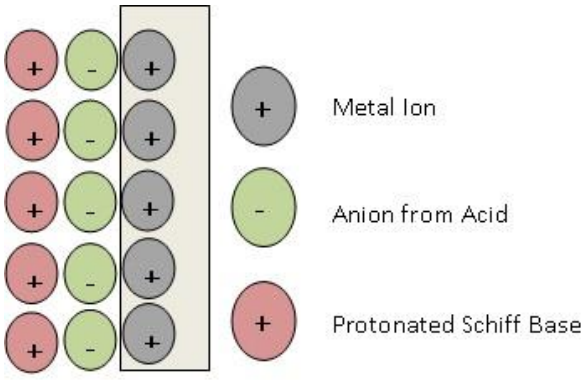

Fig.7a Arrangement of ions in the system containing the inhibitor

JCSE The Journal of Corrosion Science and Engineering
ISSN 1466-8858 Volume 23, Paper 50 first submitted 21 September 2020
published 19 September 2021

3.5 ADSORPTION ISOTHERM

The adsorption of synthesized Schiff base molecules onto the metal surface could be explained on the basis of adsorption isotherm. Generally, adsorption is considered as substitution process where the molecules of water adsorbed onto the metal surface are replaced by inhibitor molecules and this process can be represented as [32],

$$Org_{sol} + xH_2O_{ads} \leftrightarrow Org_{ads} + xH_2O \quad (6)$$

where 'x' represents the number of water molecules replaced by Schiff base molecule. Based on the surface coverage and corrosion inhibition efficiency of BIS, the mechanism for the adsorption of this inhibitor molecule onto the mild steel surface can be described.

In the present case various adsorption isotherms had tested with the experimental data and it was found that the experimental data fit well with the Langmuir adsorption isotherm. This is shown in Fig.8a and 8b. Langmuir adsorption isotherm is given by the expression [27,32,35]

$$C_{inh}/\theta = C_{inh} + 1/K_{ads} \quad (7)$$

Where C_{inh} is the concentration of the inhibitor, θ is the surface coverage and K_{ads} is the equilibrium constant. The value of K_{ads} is determined from the plot of C_{inh}vs C_{inh}/θ at constant temperature. The value of $K_{ads}$is used to calculate the value of the standard free energy of adsorption using the following expression [32].

$$K_{ads} = 1/55.5 \exp(-\Delta G^0_{ads}/RT) \quad (8)$$

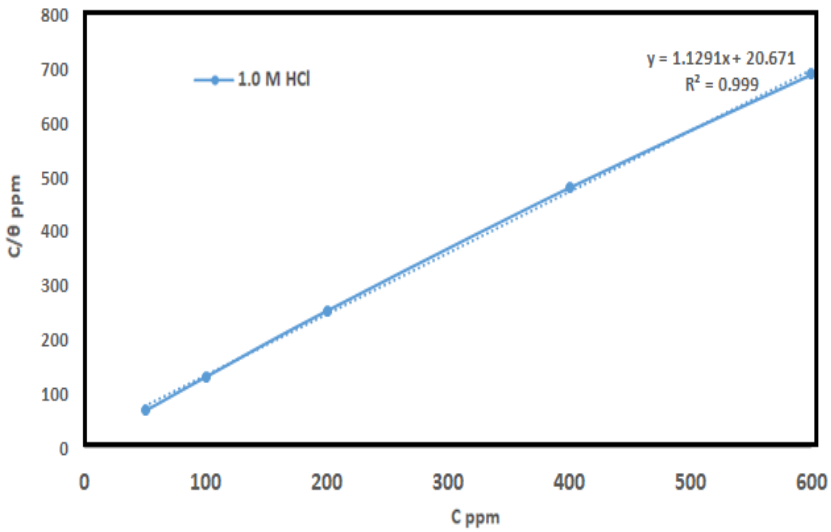

Fig.8a Langmuir's isotherm for the adsorption of the Schiff base, BIS on mild steel surface in 1.0 M HCl solution.

JCSE The Journal of Corrosion Science and Engineering
ISSN 1466-8858 Volume 23, Paper 50 first submitted 21 September 2020
published 19 September 2021

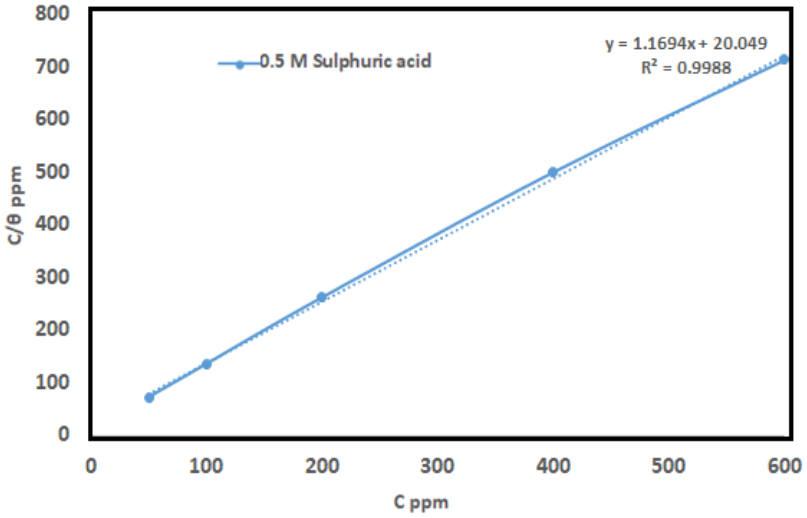

Fig.8b Langmuir's isotherm for the adsorption of the Schiff base, BIS on mild steel surface in 0.5 M H_2SO_4 solution.

The adsorption isotherms are linear with the correlation coefficients greater than 0.9. The standard free energy change(ΔG^0_{ads}) values calculated from the adsorption isotherm in 1.0 M HCl and 0.5 M H_2SO_4 solutions are -46.82 kJmol^{-1} and -44.14 kJmol^{-1} respectively. The negative sign of standard free energy of adsorption indicated the spontaneous adsorption of inhibitor molecules onto the metal surface. In general the value of $-\Delta G^0_{ads}$ is less than to 20 kJmol^{-1}, the inhibitor molecules are said to be adsorbed by physisorption mechanism [32]. If the value of $-\Delta G^0_{ads}$ is greater than 40 kJmol^{-1}, then it would represent adsorption of inhibitor molecules onto the metal surface primarily by chemisorption [32]. On the other hand if this value is in between 20 and 40 kJmol^{-1}, then it indicates the adsorption of inhibitor molecules on the metal surface involves both physisorption and chemisorption [30,32]. In the present case the $-\Delta G^0_{ads}$ for the adsorption of inhibitor molecules on the mild steel surface is greater than 40 kJ mol^{-1} indicating the adsorption of inhibitor molecules onto the mild steel surface primarily caused by chemisorption [32].

3.6 EFFECT OF TEMPERATURE

Nyquist plots recorded for the corrosion of mild steel in 1.0 M HCl and 0.5 M H_2SO_4 solutions in the absence and presence of BIS at various temperatures were shown in fig. 9a to 9d. The charge transfer

JCSE The Journal of Corrosion Science and Engineering
ISSN 1466-8858 Volume 23, Paper 50 first submitted 21 September 2020
published 19 September 2021

resistance values extracted from the Nyquist plots using the equivalent circuit shown in Figure. 4 are presented in Table.5. and 6.

The Arrhenius type of plots obtained by plotting log(1/Rct) against 1/Temperature in 0.1 M HCl and 0.5 M H_2SO_4 in the absence and presence of the synthesized Schiff base are shown in Fig. 10a and 10b.

$$\log(1/Rct) \alpha \log(\text{corrosion rate}) = -Ea/2.303R\ (1/T) + \log A \qquad (9)$$

The energy of activation values calculated from the Arrhenius plots are presented in Table.7. The decrease in energy of activation with the addition of inhibitor to the acid solutions implied a different mechanism for the corrosion of mild steel in the presence of the inhibitor molecules [30]. It is well known that an increase in temperature will influence the kinetics adsorption of inhibitor molecules onto the metal surface and also adsorption equilibria [33].The decrease in energy of activation in the presence of inhibitor molecules in the corrosive media was explained in different ways in literature [30,34-38]. At high temperatures, the surface area covered by the inhibitor molecules increases and the rate of metal dissolution in the corrosive media is controlled by diffusion of the corrosion product through the inhibitor's protective film [39]. Some authors enunciated that the overall rate of metal dissolution is caused by the corrosion of the bare metal surface and the corrosion of surface covered by the inhibitor molecules [30]. In the present work the corrosion of metal surface could be less at the high degree of surface coverage. This led to conclude that at high degree of surface coverage the interaction is between the metal surface and inhibitor molecules. In such a case, the activation energy can be smaller or higher than in the absence of inhibitor molecules [40]. Other authors [41-44] suggest that the lower activation energy in the presence of inhibitor molecules is an indication of chemisorption of the inhibitor molecules onto the metal surface.

JCSE The Journal of Corrosion Science and Engineering
ISSN 1466-8858 Volume 23, Paper 50 first submitted 21 September 2020
published 19 September 2021

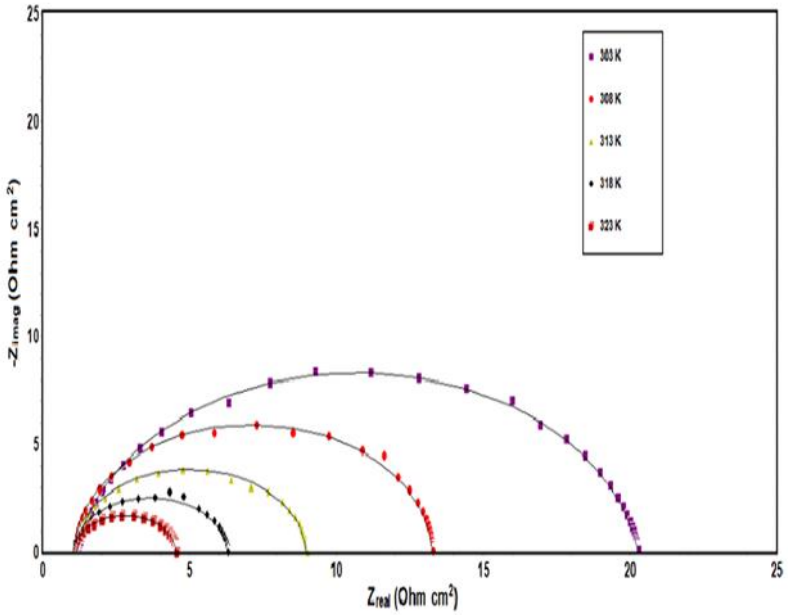

Fig.9a Nyquist plots recorded for the corrosion of mild steel in 1.0 M HCl solutions in the absence of BIS at various temperature.

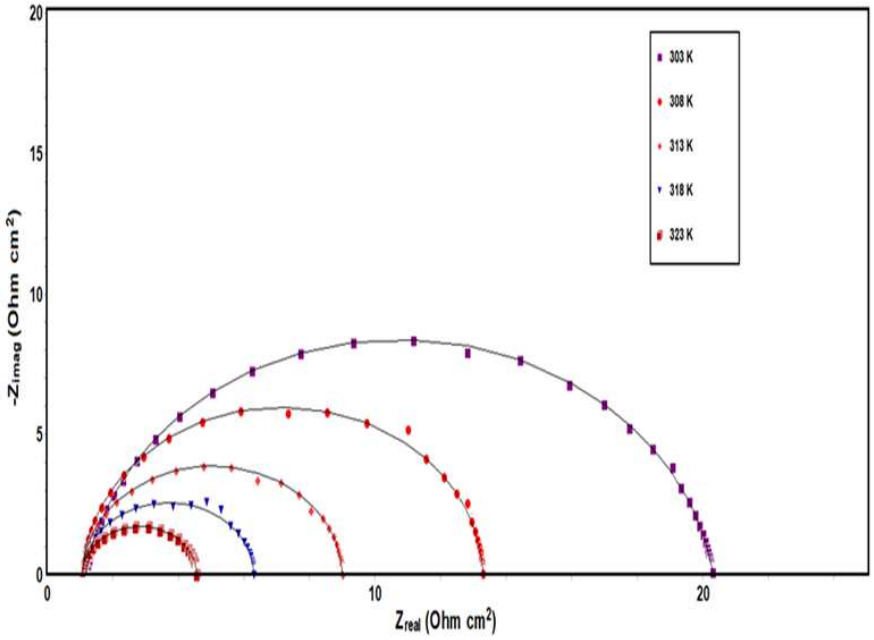

Fig.9b Nyquist plots recorded for the corrosion of mild steel in 0.5 M H_2SO_4 solutions in the absence of BIS at various temperature.

JCSE The Journal of Corrosion Science and Engineering
ISSN 1466-8858 Volume 23, Paper 50 first submitted 21 September 2020
published 19 September 2021

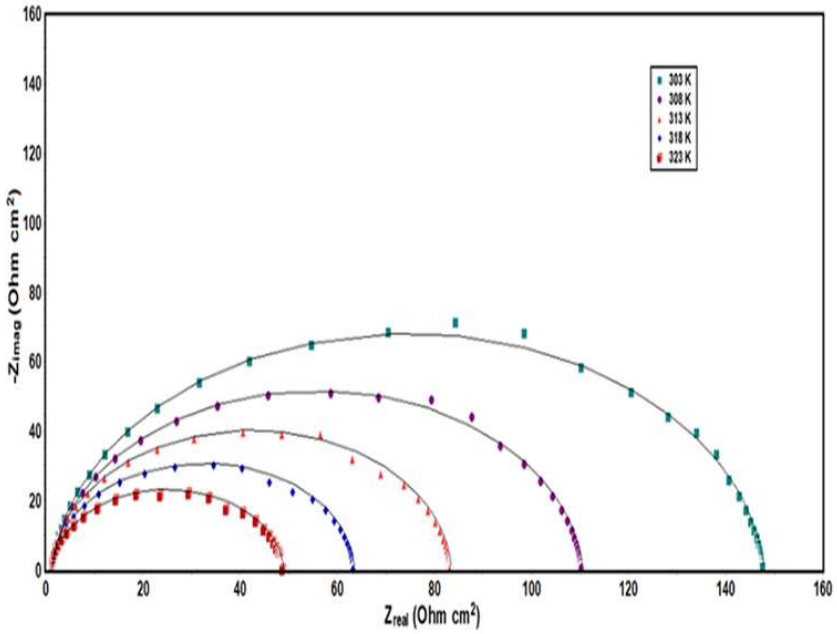

Fig.9c Nyquist plots recorded for the corrosion of mild steel in 1.0 M HCl solutions in the presence of BIS at various temperature.

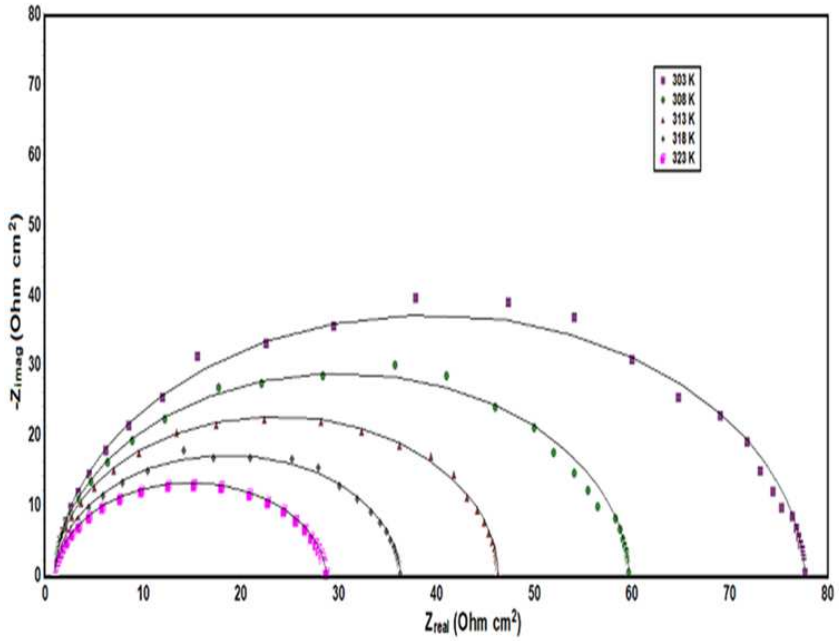

Fig.9d Nyquist plots recorded for the corrosion of mild steel in 0.5 M H_2SO_4 solutions in the presence of BIS at various temperature.

JCSE The Journal of Corrosion Science and Engineering
ISSN 1466-8858 Volume 23, Paper 50 first submitted 21 September 2020
published 19 September 2021

Table.5 Energy of activation for the corrosion of mild steel in 1.0 M HCl and 0.5 M H_2SO_4 solutions in the absence and presence of BIS

S.No.	Medium	Energy of activation (kJ mol^{-1})
1	1.0 M HCl	69.13
2	0.5 M H_2SO_4	61.23
3	1.0 M HCl + 600 ppm of inhibitor	45.78
4	0.5 M H_2SO_4 + 600 ppm of inhibitor	41.44

Table.6 Effect of temperature on the corrosion of mild steel in 1.0 M HCl and 0.5 M H_2SO_4 solutions in the absence of the Schiff base BIS.

S.No.	Temperature (K)	Charge transfer resistance (Ohm cm^2)	
		1.0 M HCl	0.5 M H_2SO_4
1	303	19.1	12.5
2	308	12.2	8.23
3	313	7.92	5.66
4	318	5.23	3.93
5	323	3.49	2.76

JCSE The Journal of Corrosion Science and Engineering
ISSN 1466-8858 Volume 23, Paper 50 first submitted 21 September 2020
published 19 September 2021

Table.7 Effect of temperature on the corrosion of mild steel in 1.0 M HCl and 0.5 M H_2SO_4 solutions in the presence of the Schiff base BIS

S.No.	Temperature (K)	Charge transfer resistance (Ohm cm^2)	
		1.0 M HCl + 600 ppm inhibitor	0.5 M H_2SO_4 + 600 ppm inhibitor
1	303	146.6	76.7
2	308	109.2	58.7
3	313	82.1	45.3
4	318	62.2	35.3
5	323	47.6	27.7

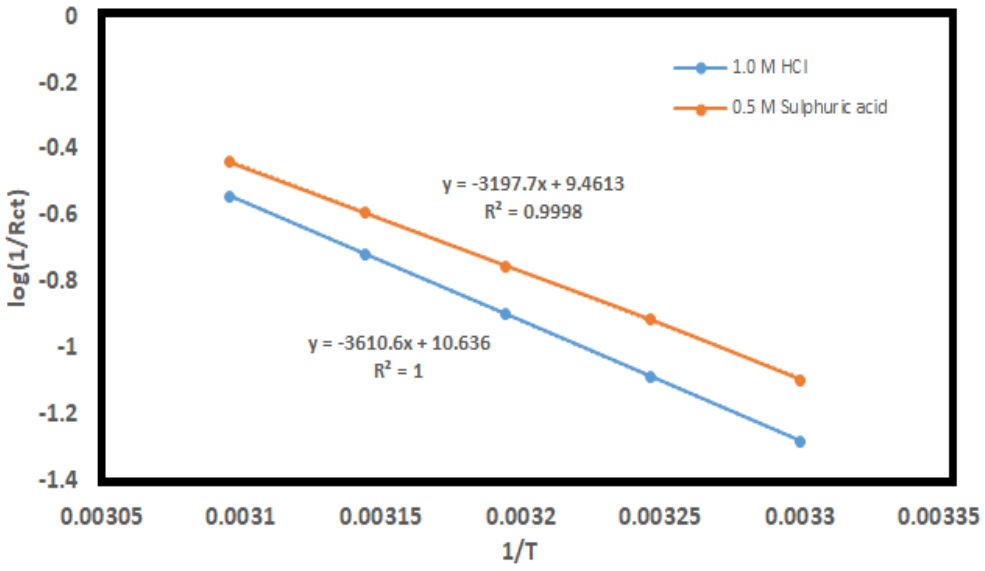

Fig.10a Arrhenius type plot on corrosion of mild steel in 1.0 M HCl and 0.5 M H_2SO_4 solutions in the absence of BIS with different temperatures.

JCSE The Journal of Corrosion Science and Engineering
ISSN 1466-8858 Volume 23, Paper 50 first submitted 21 September 2020
published 19 September 2021

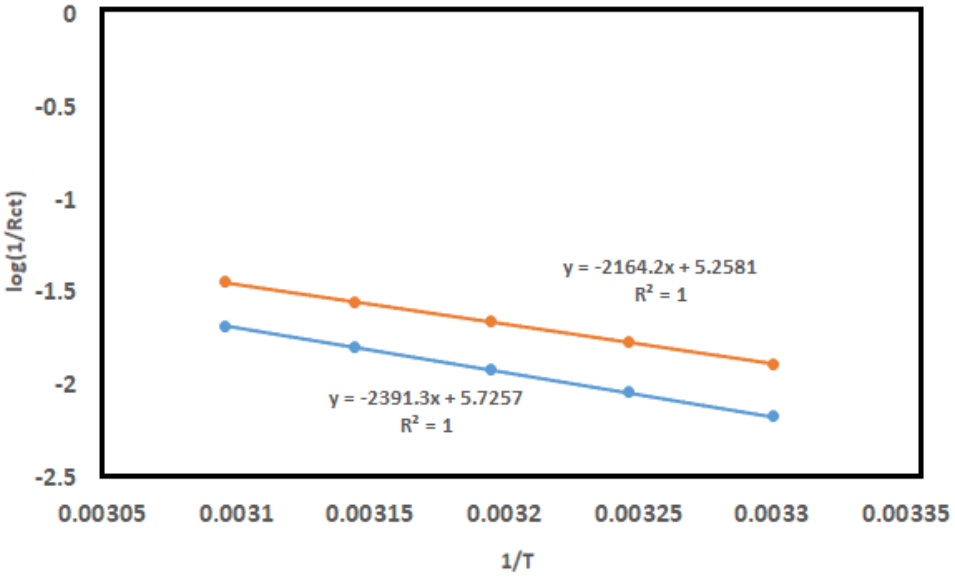

Fig.10b Arrhenius type plot on corrosion of mild steel in 1.0 M HCl and 0.5 M H_2SO_4 solutions in the presence of BIS with different temperatures.

3.7 QUANTUM CHEMICAL CALCULATIONS ON MOLECULAR PROPERTIES OF SCHIFF BASE AND ITS PROTONATED FORM

The molecular parameters of Schiff base and its protonated form were evaluated using quantum chemical calculations. The quantum chemical calculations were made using optimized structures of Schiff base and its protonated forms. The quantum chemical parameters calculated are presented in Table 8.

The electron density in the neutral and protonated Schiff base molecules are represented by HOMO and LUMO structures in Fig.11-18.

JCSE The Journal of Corrosion Science and Engineering
ISSN 1466-8858 Volume 23, Paper 50 first submitted 21 September 2020
published 19 September 2021

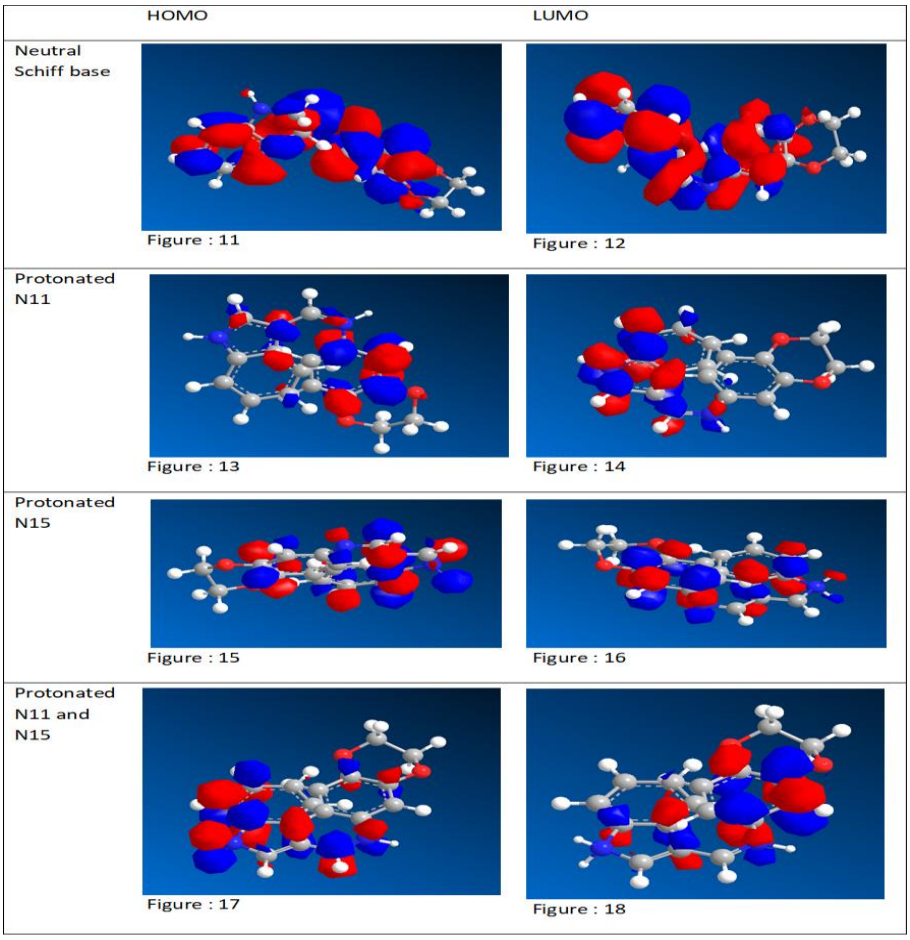

Fig.11-18. HOMO and LUMO of synthesized Schiff base and its protonated forms

JCSE The Journal of Corrosion Science and Engineering
ISSN 1466-8858 Volume 23, Paper 50 first submitted 21 September 2020
published 19 September 2021

Table. 8 Molecular Properties derived from Quantum Chemical descriptors for N-((1H-indol-3yl)methylene)-2,3dihydrobenzo[b] [1,4] dioxin-6-amine and its protonated forms in acid solution using DFT.

S.No.	QC Parameters	Neutral molecule	Protonated at N-11	Protonated at N-15	Protonated at N-11 and N-15
1.	Total energy (eV)	-3238.49357	-3252.1917	-3250.59772	-3264.15392
2.	E_{HOMO} (eV)	-8.264	-8.04	-7.803	-6.31
3.	E_{LUMO} (eV)	-0.514	-0.28	-0.367	-0.601
4.	ΔE (eV)	7.75	7.76	7.436	5.709
5.	Ionization Potential (I/eV)	8.264	8.04	7.803	6.31
6.	Electron affinity (A/eV)	0.514	0.28	0.367	0.601
7.	Hardness (η/eV)	3.875	3.88	3.718	2.8545
8.	Softness (S/eV)	0.129032258	0.128865979	0.134480904	0.175162025
9.	Electronegativity (χ)	4.389	4.16	4.085	3.4555
10.	Electrophilicity (ω)	2.485589806	2.230103093	2.244113098	2.091518699
11.	Fraction of electrons Transfereed (Δ N)	0.336903226	0.365979381	0.392011834	0.620861797
12.	Dipole moment	3.84995	1.48884	6.33429	6.49285

The energy of the highest occupied molecular orbital measures the tendency of the molecules to donate the electrons to the vacant lower energy orbitals of metal atoms [49]. Inspection of Table 8 reveals that E_{HOMO} value is largest for protonated form at N-11 and N-15, hence this form in acid media should show more contribution to the corrosion inhibition of mild steel. The protonated molecules may be attached to the metal surface via the positively charged nitrogen atoms through the corresponding anions of acids as discussed earlier. Now, the π electrons of >C=N- and benzene ring and O atoms in the dioxin ring are very close to metal surface and could form chemical bonding through π electrons and lone pair of electrons. The E_{HOMO} value of unprotonated Schiff base molecule is not too low, it is

JCSE The Journal of Corrosion Science and Engineering
ISSN 1466-8858 Volume 23, Paper 50 first submitted 21 September 2020
published 19 September 2021

also comparable with protonated form, hence this form might also have shown contribution to corrosion inhibition through chemisorption.

E_{LUMO} shows the ability of molecule to accept electrons. Lower the E_{LUMO}, higher will be the tendency to accept electrons from surface metal atoms. The protonated form of Schiff base at N-11 and N-15has lower E_{LUMO} than other protonated form, therefore in this form the electron acceptance tendency is high.

The energy gap (ΔE) between HOMO and LUMO reveals the reactivity of molecule for the adsorption onto the metal surface [50]. As the energy gap (ΔE) decreases, the reactivity of the molecular species increases. The energy gap is lower for protonated form of Schiff base molecule at N-11 and N-15 than neutral form. Hence, its reactivity should be high.

Dipole moment of the molecular species, which is a measure of polarity and polar bonds, also determines the electron distribution in the molecular species [51]. Literature review revealed that the corrosion inhibition nature of molecules increased with increase in dipole moment [50,51]. In the present case protonated form of Schiff base molecule at N-11 and N-15shows the higher value for dipole moment. Therefore, this form should show more contribution to corrosion inhibition efficiency than neutral molecule and other protonated forms. Higher the value of ionization energy for a molecular species, higher will be stability and lower the reactivity or higher the chemical inertness [52]. The protonated form of Schiff base molecule at N-11 and N-15has relatively lower ionization potential than neutral form, hence this form might have higher reactivity towards adsorption onto mild steel surface. Absolute hardness and softness are important properties to measure the molecular stability and reactivity. These two forms of the Schiff base have almost same value for hardness and softness and thus have same stability.

Electrophilicity index (ω) is another quantum chemical parameter measuring the tendency of inhibitor molecules to accept electrons from metal. An organic compound is said to be a potential corrosion inhibitor when it has lower electrophilicity index. Inspection of Table.8 reveals that the protonated form of Schiff base molecule at N-11 and N-15 has lower electrophilicity index than unprotonated form. Thus, the protonated form has good electron accepting tendency in addition to donation. The fraction of charge donated is also high for protonated form of Schiff base molecule at

JCSE The Journal of Corrosion Science and Engineering
ISSN 1466-8858 Volume 23, Paper 50 first submitted 21 September 2020
published 19 September 2021

N-11 and N-15 than other forms this also suggests more contribution from this form for the observed corrosion inhibition efficiency. The adsorption isotherm studies suggest chemisorption of inhibitor molecule onto the metal surface whereas the PZC and quantum chemical studies suggest that physisorption also a contributing factor for adsorption. Hence, it can be concluded that the protonated form of Schiff base molecule at N-11 and N-15 could be attached to the metal surface via chloride or sulphate bridge, bringing the molecule close to metal surface, which facilitates the formation of chemical bond between lone pair of electrons of oxygen atom and π electrons of >C=N bond and aromatic rings.

4.CONCLUSION

The following are the conclusions arrived at the present study

(i) The corrosion inhibition efficiency of the synthesized inhibitor increased with concentration in both 1.0 M HCl & 0.5 M H_2SO_4 solutions. The maximum inhibition efficiency was observed at 600 ppm .

(ii) The results of weight loss data are supported by electrochemical studies. The Tafel polarization studies show that the inhibitor is of mixed type.

(iii) The standard free energy of adsorption of inhibitor, calculated from adsorption isotherm shows that adsorption of inhibitor onto the mild steel surface in acid media is spontaneous and adsorption involves chemisorption mechanism. However, PZC studies indicated that the metal surface is positively charged in both the acid media in the presence and absence of inhibitor. In acid media the Schiff base molecules can protonate and this protonated positively charged form of Schiff base can't approach the positively charged metal surface . The counter ions (anions) of the acid can easily approach the positively charged metal surface via electrostatic forces. These ions can further attract the positively charged (protonated) Schiff base molecules from the solution via electrostatic force. In other words, protonated Schiff base molecules get adsorbed onto the carbon steel surface involves physisorption through the anion bridges.Thus, the adsorption of Schiff base molecules onto the metal surface involved both physisorption and chemisorption.

(iv) The quantum chemical calculations show that the Schiff base molecules protonated at both the nitrogen atoms might have shown more contribution to the observed corrosion inhibition efficiency than other forms.

JCSE The Journal of Corrosion Science and Engineering

ISSN 1466-8858 Volume 23, Paper 50 first submitted 21 September 2020
published 19 September 2021

REFERNCES

1. Prabhu, R. A., T. V. Venkatesha, A. V. Shanbhag, B. M. Praveen, G. M. Kulkarni, and R. G. Kalkhambkar. Materials Chemistry and Physics 108, no. 2-3, 283-289 (2008)
2. Ahamad, Ishtiaque, Rajendra Prasad, and M. A. Quraishi. Corrosion Science 52,no. 3, 933-942 (2010)
3. Amin, Mohammed A., and K. F. Khaled. Corrosion science 52, no.5, 1762-1770 (2010)
4. Raja, Pandian Bothi, Mohammad Ismail, Seyedmojtaba, Ghoreishiamiri, Jahangir Mirza, Mokhtar Che Ismail, SaeidKakooei, and Afidah Abdul Rahim. Chemical Engineering Communications 203, no. 9, 1145-1156 (2016).
5. Winkler, David Alan, Michael Breedon, Anthony E. Hughes, Frank Robert Burden, Amanda Susan Barnard, Timothy G. Harvey, and I. Cole. Green Chemistry16,no.6, 3349-3357 (2014)
6. Ahamad, Ishtiaque, Rajendra Prasad, and M. A. Quraishi Corrosion Science 52, no. 3, 933-942 (2010)
7. Bentiss, F., M. Traisnel, and M. Lagrenee. Corrosion science 42, no.1,127-146 (2000)
8. Morad, M. S. Corrosion Science 50, no. 2, 436-448 (2008)
9. Musa, Ahmed Y., Abdul Amir H. Kadhum, Abu Bakar Mohamad, MohdSobriTakriff, Abdul Razak Daud, and Siti KartomKamarudin. Corrosion Science 52, no. 2, 526-533 (2010)
10. Hasanov, Rovshan, Selen Bilge, SemraBilgiç, GökhanGece, and ZeynelKılıç.Corrosion science 52, no. 3, 984-990 (2010)
11. Hefter, G. T., N. A. North, and S. H. Tan. Corrosion 53, no. 8,657-667 (1997)
12. Ju,Hong,Zhen-PengKai, and Yan Li.Corrosion Science 50, no.3,865-871(2008)
13. Yıldırım, A., and M. Cetin Corrosion Science 50, no. 1, 155-165 (2008)
14. Fang, Jian, and Jie Li, Journal of Molecular Structure: THEOCHEM 593, no. 1-3, 179-185 (2002)
15. Obot, I. B., and N. O. Obi-Egbedi Corrosion Science 52, no. 2, 657-660 (2010)

ISSN 1466-8858 Volume 23, Paper 50 first submitted 21 September 2020
published 19 September 2021

16. Ahamad, Ishtiaque, Rajendra Prasad, and M. A. Quraishi Corrosion Science 52, no. 3, 933-942 (2010)
17. Yurt, A., A. Balaban, S. UstünKandemir, G. Bereket, and B. Erk. Materials Chemistry and Physics 85, no. 2-3, 420-426 (2004)
18. Wang, Hui-Long, Rui-Bin Liu, and Jian Xin, Corrosion Science 46, no. 10, 2455-2466 (2004)
19. Herrag, L., BelkheirHammouti, S. Elkadiri, A. Aouniti, C. Jama, H. Vezin, and F. Bentiss. Corrosion Science 52, no. 9, 3042-3051 (2010)
20. Ebenso, Eno E., Ime B. Obot, and L. C. Murulana, Int. J. Electrochem. Sci 5,1574-1586 (2010)
21. Forsyth, Maria, Kerryn Wilson, Thomas Behrsing, Craig Forsyth, Glen B. Deacon, and A. Phanasgoankar, Corrosion 58, no. 11,953-960 (2002)
22. Ferreira, E. S., C. Giacomelli, F. C. Giacomelli, and A. Spinelli.Materials Chemistry and Physics 83, no. 1,129-134 (2004)
23. Safiuddin, Md, and Nataliya Hearn. Cement and Concrete Research 35, no. 5, 1008-1013 (2005)
24. Ansari, K. R., Dileep Kumar Yadav, Eno E. Ebenso, and M. A. Quraishi, Int. J. Electro chem. Sci 7, 4780-4799 (2012)
25. Behpour, M., S. M. Ghoreishi, N. Soltani, M. Salavati-Niasari, M. Hamadanian, and A. Gandomi. Corrosion Science 50, no. 8, 2172-2181 (2008)
26. Bauschlicher Jr, Charles W., and Harry Partridge. The Journal of chemical physics 103, no. 5, 1788-1791 (1995)
27. RameshKumar, S., I. Danaee, M. RashvandAvei, and M. Vijayan. Journal of Molecular Liquids 212,168-186 (2015)
28. Ahamad, Ishtiaque, Rajendra Prasad, and Mumtaz Ahmad Quraishi. Journal of Solid State Electrochemistry 14, no. 11, 2095-2105 (2010)

ISSN 1466-8858 Volume 23, Paper 50 first submitted 21 September 2020
published 19 September 2021

29. Pavithra, M. K., T. V. Venkatesha, K. Vathsala, and K. O. Nayana. Corrosion Science 52, no. 11,3811-3819 (2010)

30. Mallaiya, Kumaravel, Rameshkumar Subramaniam, Subramanian Sathyamangalam Srikandan, S. Gowri, N. Rajasekaran, and A. Selvaraj.Electrochimica Acta 56, no. 11,3857-3863 (2011)

31. Singh, Ambrish, V. K. Singh, and M. A. Quraishi. Rasayan Journal of Chemistry 3, no. 4, 811-824 (2010)

32. Ansari, K. R., Sudheer, Ambrish Singh, and M. A. Quraishi. Journal of Dispersion Science and Technology 36, no. 7,908-917 (2015)

33. Ghasemi, O., I. Danaee, G. R. Rashed, M. RashvandAvei, and M. H. Maddahy. Journal of Central South University 20, no. 2, 301-311 (2013)

34. Solmaz, R., M. E. Mert, G. Kardaş, B. Yazici, and M. Erbil Acta Physico- ChimicaSinica 24, no. 7,1185-1191 (2008)

35. Benard, P., and R. Chahine. Langmuir 13, no. 4, 808-813 (1997)

36. Vilar, Vítor JP, Cidália MS Botelho, and Rui AR Boaventura. Process Biochemistry 40, no. 10, 3267-3275 (2005)

37. Popova, A. Corrosion Science 49, no. 5,2144-2158 (2007)

38. Gomma, Gamal K., and Mostafa H. Wahdan. Bulletin of the Chemical Society of Japan 67, no. 10, 2621-2626 (1994)

39. Solmaz, R., G. Kardaş, M. Culha, B. Yazıcı, and M. Erbil Electrochimica Acta 53,no. 20, 5941-5952 (2008)

40. Behpour, M., S. M. Ghoreishi, N. Mohammadi, N. Soltani, and M. Salavati- Niasari Corrosion Science 52, no. 12, 4046-4057 (2010)

41. Riggs Jr, Olen L., and Ray M. Hurd Corrosion 23, no. 8,252-260 (1967)

JCSE The Journal of Corrosion Science and Engineering
ISSN 1466-8858 Volume 23, Paper 50 first submitted 21 September 2020
published 19 September 2021

42. Bentiss,F,M. Traisnel, and M.Lagrenee. Corrosion science 42, no.1,127-146 (2000)

43. Z.A. Foroulis, Proceedings of 6th European Symposium on Corrosion Inhibitors, Ann. Univ. Ferrara, p. 130. (1985)

44. Szauer, T., and A. Brandt Corrosion science 23, no. 12 1247-1257 (1983)

45. Karzazi, Yasser, Mohammed El AlaouiBelghiti, Ali Dafali, and BelkheirHammouti J. Chem. Pharm. Res 6, 689-696 (2014)

46. Saha, Sourav Kr, Pritam Ghosh, Abhiram Hens, Naresh Chandra Murmu, and Priyabrata Banerjee Physica E: Low-dimensional systems and nanostructures 66, 332-341 (2015)

47. Ravi, M., T. Soujanya, A. Samanta, and T. P. Radhakrishnan Journal of the Chemical Society, Faraday Transactions 91, no. 17, 2739-2742 (1995)

48. Geerlings, Paul, F. De Proft, and W. Langenaeker. Chemical reviews 103, no. 5,1793-1874 (2003)